JACS
JOURNAL OF THE AMERICAN CHEMICAL SOCIETY

Communication

pubs.acs.org/JACS

Nucleation and Growth of Ordered Arrays of Silver Nanoparticles on Peptide Nanofibers: Hybrid Nanostructures with Antimicrobial Properties

Elena Pazos,[†,#] Eduard Sleep,[†] Charles M. Rubert Pérez,[†] Sungsoo S. Lee,[†,§] Faifan Tantakitti,[†,§,∇] and Samuel I. Stupp*[,†,‡,§,∥,⊥]

[†]Simpson Querrey Institute for BioNanotechnology, Northwestern University, Chicago, Illinois 60611, United States
[‡]Department of Chemistry, [§]Department of Materials Science and Engineering, [∥]Department of Medicine, and [⊥]Department of Biomedical Engineering, Northwestern University, Evanston, Illinois 60208, United States

Supporting Information

ABSTRACT: Silver nanoparticles have been of great interest as plasmonic substrates for sensing and imaging, catalysts, or antimicrobial systems. Their physical properties are strongly dependent on parameters that remain challenging to control such as size, chemical composition, and spatial distribution. We report here on supramolecular assemblies of a novel peptide amphiphile containing aldehyde functionality in order to reduce silver ions and subsequently nucleate silver metal nanoparticles in water. This system spontaneously generates monodisperse silver particles at fairly regular distances along the length of the filamentous organic assemblies. The metal−organic hybrid structures exhibited antimicrobial activity and significantly less toxicity toward eukaryotic cells. Metallized organic nanofibers of the type described here offer the possibility to create hydrogels, which integrate the useful functions of silver nanoparticles with controllable metallic content.

Silver nanoparticles (AgNPs) have been of great interest as plasmonic substrates for sensing and imaging,[1] and also as catalysts[2] or antimicrobial systems.[3] The properties of AgNPs depend on their size, shape, and composition as well as on their spatial arrangement.[4] Therefore, preparing stable AgNPs with defined dimensions and controlled spatial architectures is an important goal that remains a significant challenge. A number of scaffolds have been recently used for the assembly or growth of AgNPs. Thus, for example, non-natural aldehyde-modified nucleobases have been incorporated into DNA strands to promote the nucleation of AgNPs along the DNA chain;[5] peptide-based nanofibers have been used to grow silver nanoparticles through reduction with $NaBH_4$ of coordinated Ag^+ ions;[6] and nanotubes modified with nucleobases or peptides on their surface have been also employed to produce one-dimensional arrangements of AgNPs.[2b,7] However, the coverage of the organic structures is usually incomplete, the NP size distribution is typically broad, and the spatial arrangement of the NPs is irregular. Therefore, the development of efficient methods for the synthesis of hybrid structures that control these parameters is of great interest. We report here a one-pot method for the site-specific nucleation and growth of AgNPs using supramolecular nanofibers formed by peptide-amphiphiles (PAs).

PAs that form long supramolecular nanofibers were developed over the past decade and require the presence of amino acid sequences with propensity to form β-sheets in addition to hydrophobic fatty acid segments at one terminus.[8] These molecules self-assemble in aqueous solution to form high-aspect-ratio nanostructures, such as fibers and ribbons, in which the alkyl tails are isolated from the aqueous environment by hydrophobic collapse. Their great structural diversity and biodegradability makes them effective in the design of bioactive scaffolds,[9] drug delivery systems,[10] and targeted therapies.[11] PAs have also been used as scaffolds to direct the synthesis and assembly of nanoparticles.[12]

In this work our goal has been to design PA nanofibers with functional groups that would induce formation of AgNPs over the PA fibers. AgNPs are usually synthesized by the chemical reduction of Ag^+ salts in the presence of stabilizing additives like polymers or surfactants. However, the use of peptides have recently attracted attention for their biocompatibility and because they allow the formation of AgNPs in water.[13] We chose to use aldehyde moieties to control nucleation since this functional group is known to reduce two silver ions to form Ag_2 clusters, while simultaneously oxidizing to carboxylic acid groups (via the Tollens' reaction) without the need for an external reducing agent or additives to control the nucleation.[14] We designed **PA-1**, which is modified at the N-terminus with an aldehyde that would be exposed on the surface of the self-assembled nanofibers.

PA-1 was synthesized following standard Fmoc solid-phase procedures (Scheme 1, also see Supporting Information). The aldehyde moiety was obtained by oxidation of the 1,2-diol group with sodium periodate in aqueous solution. We also synthesized a control PA that lacks the aldehyde functional group (**PA-2**).

We first studied the capacity of **PA-1** and **PA-2** to self-assemble into supramolecular nanofibers using transmission electron microscopy (TEM). As expected based on their peptide sequences, both PAs formed high-aspect-ratio nanofibers in aqueous solution (Figure S4). The PA fibers (0.5 mM

Received: February 11, 2016
Published: April 22, 2016

DOI: 10.1021/jacs.6b01570
J. Am. Chem. Soc. 2016, 138, 5507−5510

Scheme 1. Synthesis of PA-1

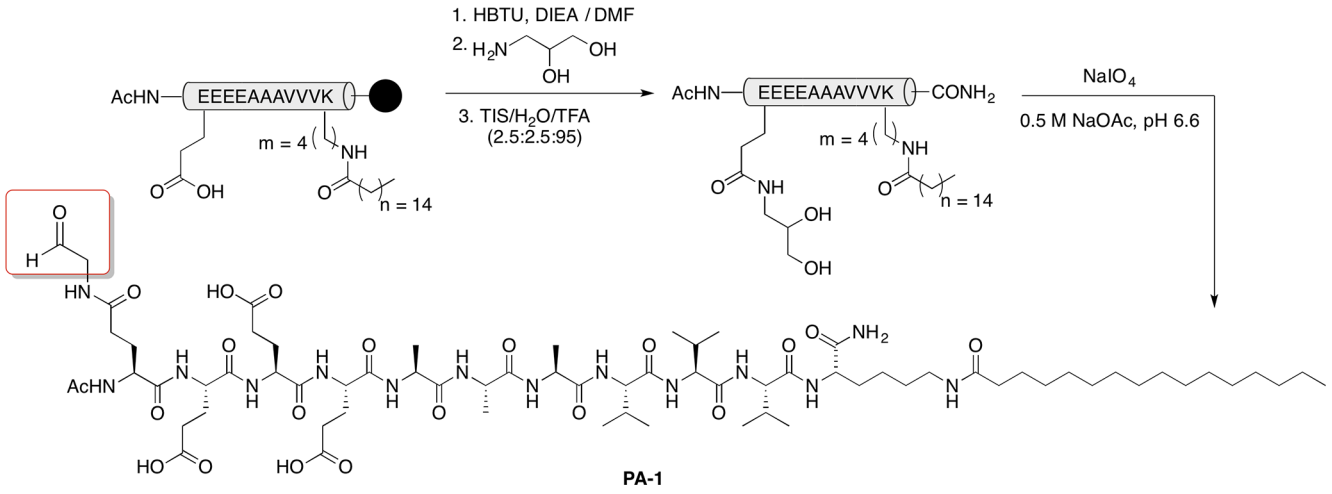

PA monomer) were then treated with Tollens' solution (final concentrations: 1 mM $AgNO_3$, 1.2 mM NaOH, 4.3 mM NH_4OH), which immediately turned the **PA-1** solution yellow. The formation of AgNPs was monitored by UV–vis spectroscopy following their characteristic plasmon absorption band between 400 and 450 nm. Moreover, this band was only observed when **PA-1** was treated with Tollens' solution, almost reaching an equilibrium absorbance value 6 h after the addition of the reagent (Figure 1a; Figures S1, S2, and S3).

In order to analyze the resulting **PA-1–AgNPs** structures, we deposited on a carbon coated copper grid the solutions after the addition of Tollens' reagent and without purification, and then dried them for TEM analysis. Initial experiments with high silver concentrations showed large aggregates, which were not present when the amount of silver was reduced to the stoichiometric concentration with respect to the aldehyde. In this case, the TEM images revealed discrete AgNPs that were 2.96 ± 0.85 nm in diameter and were spatially ordered along the long axes of PA fibers (Figure 1b). We envisioned that the negatively charged surface of the peptide nanofiber, resulting from the glutamic acid residues at the N-terminus of the peptide sequence, may attract and coordinate silver ions onto the nanofiber surface, which are then reduced by the aldehydes yielding AgNPs with homogeneous size. The spatial distribution of these AgNPs remained almost constant after 1 week in water. After the addition of 5 equiv of silver to these aged solutions, the TEM images revealed a change in the diameter of the AgNPs to 4.56 ± 2.11 nm (Figures S5 and S6). These results suggest that the growth and spatial distribution of the AgNPs are controlled by the PA nanofiber. We therefore propose that the initial silver clusters fuse into larger nanoparticles aided by rearrangement of PA molecules within the supramolecular structure. The observed monodispersity should then be controlled by competing interactions of various types. For example, cohesive forces and electrostatic repulsion among PA molecules, as well as the interactions of carboxylate groups in Glu residues grouped at the N-terminus with the AgNP surface (Figure 2). There is evidence from previous work using electron paramagnetic resonance that sufficient local dynamics would allow such rearrangements.[15] The ordered distribution of AgNPs on the nanofibers, however, is likely to arise as the system minimizes electrostatic repulsion among neighboring AgNPs–PA aggregates. Similar electrostatic effects have been suggested for the arrangement of AuNPs over positively charged supramolecular nanotubes.[16] Furthermore, the metallized nanofibers were stable upon dilution, as fibers with AgNPs on their surface could be observed by TEM following a 10-fold (Figure S8) or a 500-fold (Figure S11) dilution. Under these conditions the plasmon absorption band can be observed by UV–vis spectroscopy (Figure S10). When **PA-1** is diluted to the same concentration (1 μM) before the addition of Tollens' reagent, one does not observe fibers or AgNPs by TEM or UV–vis, demonstrating that the nanofiber is critical for the formation of the AgNPs, and at the same time it is interesting that the AgNPs have a stabilizing effect on the PA supramolecular structure. Circular dichroism experiments confirmed that the secondary structure of the **PA-1** assemblies remains intact after treatment of nanofibers with Tollens' solution (Figure S12).

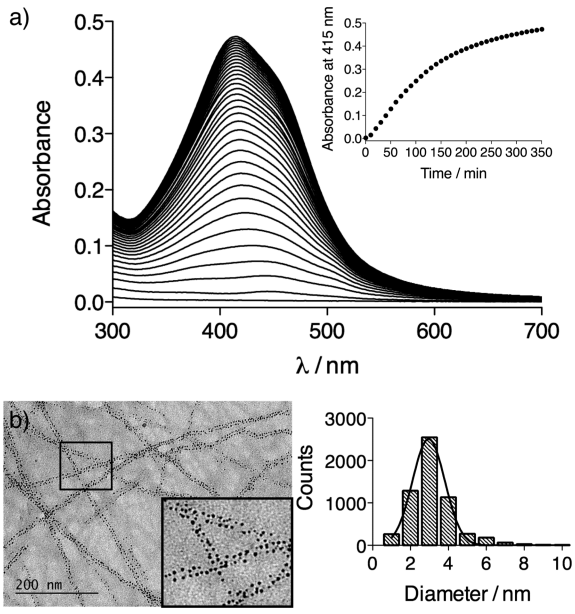

Figure 1. (a) UV–vis spectra of a 0.5 mM **PA-1** solution after the addition of Tollens' reagent (final concentrations: 1 mM $AgNO_3$, 1.2 mM NaOH, 4.3 mM NH_4OH). Inset: Absorbance of **PA-1** at 415 nm after addition of Tollens' solution versus time. (b) Representative TEM image of **PA-1–AgNPs** (0.5 mM **PA-1**, 1 mM silver) and size distribution of the AgNPs.

DOI: 10.1021/jacs.6b01570
J. Am. Chem. Soc. 2016, 138, 5507–5510

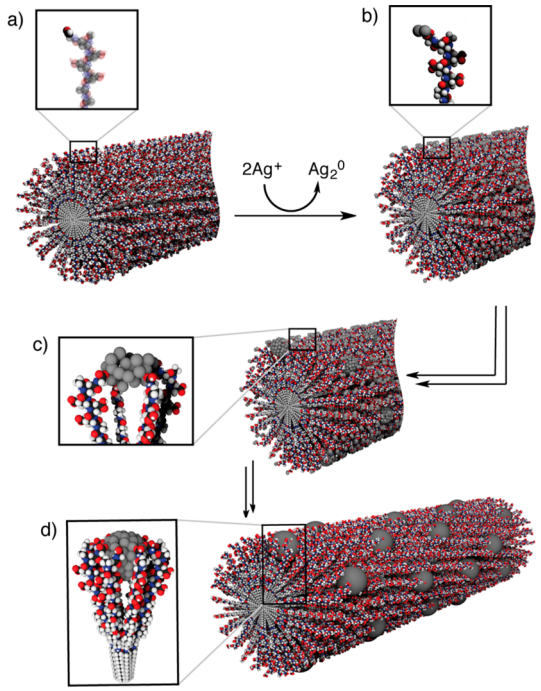

Figure 2. Formation of AgNPs over a PA nanofiber: (a) **PA-1** nanofiber displaying on its surface aldehyde functions; (b) formation of Ag_2 clusters over the **PA-1** nanofiber after the addition of Tollens' reagent; (c,d) fusion of silver clusters into larger nanoparticles, stabilized by the Glu residues.

There is currently great interest in strategies to create materials or coatings with antimicrobial properties, particularly in the context of bacterial resistance to standard antibiotics.[17] Since this type of bioactivity is well-known for AgNPs, which have been used as coatings for medical devices to prevent implant-related infections,[18] we investigated the antibacterial properties of the metallized PA nanofibers. We first investigated how bacteria respond to our system in solution. Lurie Broth (LB) medium inoculated with *E. coli* was treated with metallized nanofibers or PA nanofibers, and bacterial growth was recorded by measuring the optical density of the cultures. Treatment of bacteria with metallized nanofibers inhibited their growth, while treatment with PA nanofibers did not (Figure 3 left; Figures S13 and S17). The fractional area under the growth curve for each concentration of metallized nanofibers was fitted using a modified Gompertz function[19] to obtain the minimum inhibitory concentration (MIC) and noninhibitory concentration (NIC) values of 1.48 and 0.56 μM, respectively (Figure S14). Control experiments with bacteria treated with $AgNO_3$ in solution confirmed that metallized nanofibers have a comparable bacteriostatic effect to $AgNO_3$ (MIC = 1.22 μM and NIC = 0.52 μM, Figures S15 and S16). The toxicity of metallized nanofibers toward C2C12 cells (mouse myoblast cell line) was also tested, and we found that these nanostructures are more than 30 times less toxic to eukaryotic cells than to bacteria, and more importantly, that metallized nanofibers are less toxic to eukaryotic cells than $AgNO_3$ alone (Figure S18).

Since PA nanofibers are able to form hydrogels beyond a given concentration, the metallized fibers have potential to form antimicrobial materials. We therefore investigated if the metallized nanofibers could form gels by pipetting them (13 mM **PA-1** and 26 mM silver solution, see Supporting Information) into a 40 mM $CaCl_2$ solution. Since the

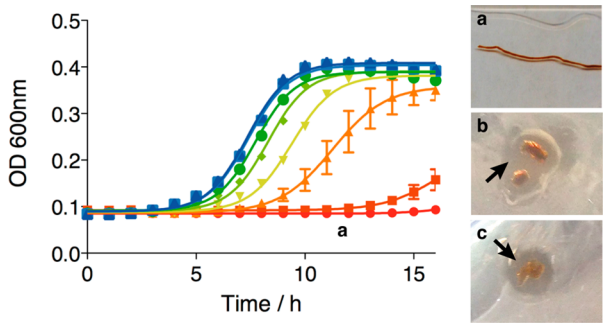

Figure 3. (left) Bacterial growth inhibition profile for *E. coli* up to 16 h in the presence of metallized nanofibers. Silver concentrations from left to right: 0, 100, 250, 500, 750 nM; 1, 1.5, and 2 μM. (right) (a) Photograph of a string-shaped metallized nanofiber gel extruded from a pipet (13 mM **PA-1**, 26 mM silver). (b,c) Photographs of an *E. coli* layer grown over an LB-agar plate, 16 h after being treated with metallized nanofiber gels. A transparent region (indicated by the arrows) around the gels delineates an inhibition zone in an otherwise opaque bacterial layer.

metallized nanofibers gelled immediately after contact with the $CaCl_2$ solution (Figure 3a; Figure S19), we tested if the resulting gels retained antimicrobial properties. A confluent layer of bacteria (*E. coli*) adsorbed over an LB-agar plate was incubated with pieces of metallized nanofiber gels at 37 °C for 16 h and tested using the agar diffusion method.[20] After the incubation period, the area surrounding the gel was examined and found to inhibit bacterial growth. We observed that this inhibition of bacterial growth occurred around the gels in all samples tested (Figure 3b,c).

We have shown here that aldehyde functionalized PA molecules form supramolecular nanofibers capable of nucleating uniformly sized and spatially ordered AgNPs in water. We further demonstrated that these metallized nanofibers have bacteriostatic effects against *E. coli* to the same degree as $AgNO_3$ in solution and low toxicity toward eukaryotic cells. Moreover, the bacteriostatic properties are retained in hydrogels of metallized nanofibers. Therefore, these metallized nanofibers offer the possibility to create hydrogels and surface films that could be useful for applications in medicine.

■ ASSOCIATED CONTENT

Supporting Information

The Supporting Information is available free of charge on the ACS Publications website at DOI: 10.1021/jacs.6b01570.

Synthetic procedures, spectroscopic and microscopic characterization, bacteriostatic assays, and cell toxicity assays (PDF)

■ AUTHOR INFORMATION

Corresponding Author

*s-stupp@northwestern.edu

Present Addresses

[#]Centre Tecnològic de la Química de Catalunya, Carrer de Marcel·lí Domingo s/n, 43007 Tarragona, Spain.

[▽]Department of Mechanical Engineering, Faculty of Engineering, Chiang Mai University, 239 Huay Kaew Rd., Muang District, Chiang Mai 50200, Thailand.

Notes

The authors declare no competing financial interest.

DOI: 10.1021/jacs.6b01570
J. Am. Chem. Soc. 2016, 138, 5507−5510

■ ACKNOWLEDGMENTS

Synthesis of PAs and their characterization were supported by the U.S. Department of Energy, Office of Science, Basic Energy Sciences, under Award Number DE-FG02-00ER45810. Biological studies were supported by National Institutes of Health NIDCR award 5 R01 DE015920. E.P., C.M.R.P., and F.T. are grateful for support by the Fundación Barrié postdoctoral fellowship, the National Institutes of Health NIBIB supplement award (3R01EB003806-09S1), and the Royal Thai scholarship, respectively. We acknowledge the following Northwestern University facilities: Peptide Synthesis and Analytical BioNanoTechnology Equipment Cores of the Simpson Querrey Institute, which have received support from the U.S. Army Research Office, the U.S. Army Medical Research and Materiel Command, and Northwestern University; Integrated Molecular Structure Education and Research Center, which has received support from the State of Illinois and the International Institute for Nanotechnology; Keck Biophysics Facility; and EPIC (NUANCE Center-Northwestern University), which has received support from the MRSEC program (NSF DMR-1121262) at the Materials Research Center; the Nanoscale Science and Engineering Center (NSF EEC-0647560) at the International Institute for Nanotechnology; and the State of Illinois, through the International Institute for Nanotechnology, for instrument use. The authors thank L. Palmer for helpful discussions and M. Seniw for graphical assistance.

■ REFERENCES

(1) (a) Polavarapu, L.; Pérez-Juste, J.; Xu, Q.-H.; Liz-Marzán, L. M. *J. Mater. Chem. C* **2014**, *2*, 7460. (b) Yao, J.; Yang, M.; Duan, Y. *Chem. Rev.* **2014**, *114*, 6130. (c) Zeng, S.; Baillargeat, D.; Ho, H.-P.; Yong, K.-T. *Chem. Soc. Rev.* **2014**, *43*, 3426.

(2) (a) Kundu, S. *Phys. Chem. Chem. Phys.* **2013**, *15*, 14107. (b) Singh, P.; Lamanna, G.; Ménard-Moyon, C.; Toma, F. M.; Magnano, E.; Bondino, F.; Prato, M.; Verma, S.; Bianco, A. *Angew. Chem., Int. Ed.* **2011**, *50*, 9893.

(3) (a) Rai, M.; Yadav, A.; Gade, A. *Biotechnol. Adv.* **2009**, *27*, 76. (b) Rizzello, L.; Pompa, P. P. *Chem. Soc. Rev.* **2014**, *43*, 1501.

(4) (a) Wiley, B.; Sun, Y.; Xia, Y. *Acc. Chem. Res.* **2007**, *40*, 1067. (b) Nie, Z.; Petukhova, A.; Kumacheva, E. *Nat. Nanotechnol.* **2010**, *5*, 15.

(5) Wirges, C. T.; Timper, J.; Fischler, M.; Sologubenko, A. S.; Mayer, J.; Simon, U.; Carell, T. *Angew. Chem., Int. Ed.* **2009**, *48*, 219.

(6) Wang, Y.; Cao, L.; Guan, S.; Shi, G.; Luo, Q.; Miao, L.; Thistlethwaite, I.; Huang, Z.; Xu, J.; Liu, J. *J. Mater. Chem.* **2012**, *22*, 2575.

(7) Yu, L.; Banerjee, I. A.; Matsui, H. *J. Am. Chem. Soc.* **2003**, *125*, 14837.

(8) (a) Hartgerink, J. D.; Beniash, E.; Stupp, S. I. *Science* **2001**, *294*, 1684. (b) Hartgerink, J. D.; Beniash, E.; Stupp, S. I. *Proc. Natl. Acad. Sci. U. S. A.* **2002**, *99*, 5133. (c) Cui, H.; Muraoka, T.; Cheetham, A. G.; Stupp, S. I. *Nano Lett.* **2009**, *9*, 945. (d) Tantakitti, F.; Boekhoven, J.; Wang, X.; Kazantsev, R.; Yu, T.; Li, J.; Zhuang, E.; Zandi, R.; Ortony, J. H.; Newcomb, C. J.; Palmer, L. C.; Shekhawat, G. S.; Olvera de la Cruz, M.; Schatz, G. C.; Stupp, S. I. *Nat. Mater.* **2016**, *15*, 469.

(9) (a) Silva, G. A.; Czeisler, C.; Niece, K. L.; Beniash, E.; Harrington, D. A.; Kessler, J. A.; Stupp, S. I. *Science* **2004**, *303*, 1352. (b) Webber, M. J.; Tongers, J.; Newcomb, C. J.; Marquardt, K. T.; Bauersachs, J.; Losordo, D. W.; Stupp, S. I. *Proc. Natl. Acad. Sci. U. S. A.* **2011**, *108*, 13438.

(10) (a) Matson, J. B.; Stupp, S. I. *Chem. Commun.* **2011**, *47*, 7962. (b) Conda-Sheridan, M.; Lee, S. S.; Preslar, A. T.; Stupp, S. I. *Chem. Commun.* **2014**, *50*, 13757. (c) Soukasene, S.; Toft, D.; Moyer, T.; Lu, H.; Lee, H.-K.; Standley, S.; Cryns, V.; Stupp, S. I. *ACS Nano* **2011**, *5*, 9113.

(11) (a) Moyer, T. J.; Kassam, H. A.; Bahnson, E. S. M.; Morgan, C. E.; Tantakitti, F.; Chew, T. L.; Kibbe, M. R.; Stupp, S. I. *Small* **2015**, *11*, 2750. (b) Bahnson, E. S. M.; Kassam, H. A.; Moyer, T. J.; Jiang, W.; Morgan, C. E.; Vercammen, J. M.; Jiang, Q.; Flynn, M. E.; Stupp, S. I.; Kibbe, M. R. *Antioxid. Redox Signaling* **2016**, *24*, 401.

(12) (a) Sone, E. D.; Stupp, S. I. *J. Am. Chem. Soc.* **2004**, *126*, 12756. (b) Li, L.-S.; Stupp, S. I. *Angew. Chem., Int. Ed.* **2005**, *44*, 1833. (c) Chen, C.-L.; Zhang, P.; Rosi, N. L. *J. Am. Chem. Soc.* **2008**, *130*, 13555. (d) Chen, C.-L.; Rosi, N. L. *J. Am. Chem. Soc.* **2010**, *132*, 6902. (e) Kim, I.; Jeong, H.-H.; Kim, Y.-J.; Lee, N.-E.; Huh, K.-M.; Lee, C.-S.; Kim, G. H.; Lee, E. *J. Mater. Chem. B* **2014**, *2*, 6478.

(13) (a) Yu, J.; Patel, S. A.; Dickson, R. M. *Angew. Chem., Int. Ed.* **2007**, *46*, 2028. (b) Rio-Echevarria, I. M.; Tavano, R.; Causin, V.; Papini, E.; Mancin, F.; Moretto, A. *J. Am. Chem. Soc.* **2011**, *133*, 8. (c) Upert, G.; Bouillère, F.; Wennemers, H. *Angew. Chem., Int. Ed.* **2012**, *51*, 4231.

(14) (a) Yin, Y.; Li, Z.-Y.; Zhong, Z.; Gates, B.; Xia, Y.; Venkateswaran, S. *J. Mater. Chem.* **2002**, *12*, 522.

(15) Ortony, J. H.; Newcomb, C. J.; Matson, J. B.; Palmer, L. C.; Doan, P. E.; Hoffman, B. M.; Stupp, S. I. *Nat. Mater.* **2014**, *13*, 812.

(16) Chhabra, R.; Moralez, J. G.; Raez, J.; Yamazaki, T.; Cho, J.-Y.; Myles, A. J.; Kovalenko, A.; Fenniri, H. *J. Am. Chem. Soc.* **2010**, *132*, 32.

(17) Campoccia, D.; Montanaro, L.; Arciola, C. R. *Biomaterials* **2013**, *34*, 8533.

(18) (a) Eckhardt, S.; Brunetto, P. S.; Gagnon, J.; Priebe, M.; Giese, B.; Fromm, K. M. *Chem. Rev.* **2013**, *113*, 4708. (b) Eby, D. M.; Luckarift, H. R.; Johnson, G. R. *ACS Appl. Mater. Interfaces* **2009**, *1*, 1553.

(19) Lambert, R. J.; Pearson, J. *J. Appl. Microbiol.* **2000**, *88*, 784.

(20) Reithofer, M. R.; Lakshmanan, A.; Ping, A. T. K.; Chin, J. M.; Hauser, C. A. E. *Biomaterials* **2014**, *35*, 7535.

DOI: 10.1021/jacs.6b01570
J. Am. Chem. Soc. 2016, 138, 5507−5510